Eco-Friendly Synthesis and Characterization of $SrBi_4Ti_{3.9}Fe_{0.1}O_{15}$ via Molten Salt Method

Nurul Fitriathus Sholikhah(✉) and Anton Prasetyo

Departement of Chemistry, Faculty Science and Technology, Universitas Islam Negeri Maulana Malik Ibrahim Malang, Jl. Gajayana 50, Malang, Indonesia 65144
nurul.fitriathus11@gmail.com

Abstract. One method of synthesizing metal oxide compounds is the molten salt method. This method is an environmentally friendly method because it does not produce waste from residual solvents and uses a lower temperature. In this research, the synthesis of the compound $SrBi_4Ti_{3.9}Fe_{0.1}O_{15}$ was carried out via the molten salt method using different salt i.e. NaCl, KCl and NaCl-KCl. The sample diffractogram shows that the compound $SrBi_4Ti_{3.9}Fe_{0.1}O_{15}$ which was synthesized using KCl and NaCl-KCl was successfully synthesized without any impurities. Meanwhile, the sample of $SrBi_4Ti_{3.9}Fe_{0.1}O_{15}$ which was synthesized with NaCl was found impurity in the form of TiO_2. The morphology of compounds synthesized using NaCl-KCl has a smaller size than compounds synthesized using salts of NaCl and KCl. The results of the calculation of the band gap energy show that the compound $SrBi_4Ti_{3.9}Fe_{0.1}O_{15}$ has a band gap energy at range ~ 2.31–2.21 eV.

Keywords: $SrBi_4Ti_{3.9}Fe_{0.1}O_{15}$ · molten salt method · Dopant Fe · morphology

1 Introduction

Photocatalyst is a process that occurs when a semiconductor material is exposed to light and then absorbs energy greater than the band gap energy; as a result, the electrons will be excited towards the conduction band and leave a hole in the valence band [1]. The photocatalyst method has advantages, such as it does not use additional chemicals and can use sun light [2].

One class of compounds reported to be used as photocatalyst materials are is Aurivillius structure. $SrBi_4Ti_4O_{15}$ compound is one of the four Aurivillius structure family that can be used as a photocatalyst with a band gap energy of 3.02 eV (410 nm) [3]. Decreasing the band gap energy will benefit its utilization as a photocatalyst material. One method that can be used is metal doped to photocatalyst compounds such as Fe metal [4].

The compounds by adding Fe dopant can be increase the photocatalyst activity. Kanakaraju et al. (2019) reported TiO_2 with Fe-doped successfully degraded methyl orange until 82.8% under UV light exposure and 74.4% under visible light exposure at optimum condition of 5 ppm initial concentration, 0.20 g of dosage and 2 h of contact

E. Susanti et al. (Eds.): ICGT 2022, AER 221, pp. 255–263, 2023.
https://doi.org/10.2991/978-94-6463-148-7_26

time. The doping of Fe into TiO_2 was able to overcome the poor photocatalytic activity of bare TiO_2 under the visible light which is only 11%.

The photocatalyst activity of an Aurivillius compound is also influenced by its particle morphology. Chen, et al. (2016) reported that the nanosheet $Bi_4Ti_3O_{12}$ can degrade rhodamine B six times faster due to has a large surface area, distinctive particle shape, small particle size, and uniform shape as a result giving good photocatalytic activity [10]. $Bi_4Ti_3O_{12}$ nanosheets with a large morphology can be degrade 80% of rhodamine B [16].

One of the most widely used synthesis methods for solid compounds is molten salt synthesis (MSS). This method is considered efficient for synthesizing metal oxide compounds and is quite simple in practice, and produces a good morphology with uniform shape and size. Therefore, the molten salt method provides an advantage for photocatalyst compound synthesis [6]. In addition, The MSS is an environmentally friendly synthesis method because it uses a relatively low temperature and does not produce hazardous waste. The type of salt used in MSS is very important, the type of salt can given the effect of the morphology, photocalyst activity, purity and other. Therefore, selection of salt used in MSS must have low melting point, high aqueous solubility and compatibility with reactants. The types of salt commonly used in MSS include nitrate, sulfate, hydroxide and chloride. The salt used in MSS [6].

Many researchers synthesized Aurivillius compounds using the MSS [7]. Synthesized using MSS can control the morphological of the sample. Zhao et al. (2014) reported MSS can give the plate-like morphology, so it's can increase of the photocatalys activity [17]. Therefore this research, we synthesized Fe-doped $SrBi_4Ti_4O_{15}$ ($SrBi_4Ti_{3.9}Fe_{0.1}O_{15}$) using MSS with various salt i.e.: NaCl, KCl, and NaCl-KCl, and then studies by (a) *X*-ray diffraction (XRD) technique, (b) scanning electron microscopy (SEM), and (c) diffuse reflectance spectroscopy (DRS).

2 Research Method

2.1 Material

The materials used in this research were $SrCO_3$ (Sigma-Aldrich, 99.9%), Bi_2O_3 (Himedia, 99.9%), TiO_2 (Sigma-Aldrich, 99.9%), Fe_2O_3 (Himedia, 99.9%), NaCl (Merck, 99%), KCl (Merck 99,9%), $AgNO_3$ (Merck, 100%).

2.2 *Synthesis of $SrBi_4Ti_{3.9}Fe_{0.1}O_{15}$ with Molten Salt Synthesis Method*

The target compound of $SrBi_4Ti_{3.9}Fe_{0.1}O_{15}$ is 3 g. In comparison, the ratio mol of the target compound and salt is 1:7. The weight requirement of materials is calculated based on stoichiometrically. All precursors and salt were ground using an agate mortar for 1 h, and acetone was added to homogenize the sample. Then the sample was heated at a temperature of 825 and 850 °C for 8 h. After that, the sample washing using hot distillate water to remove the salt in the sample and checked using $AgNO_3$ to ensure sample is salt content free. Then drying the sample with oven at temperature 90 °C for 3 h.

2.3 Characterization

The samples obtained were characterized using *X*-ray diffraction (XRD) to determine the purity and phase of the sample. Measurements were made in the range of 2θ (°) = 3–90, then the results of the diffractogram were refined using the Reitica software with the Le-Bail method. The sample's morphology was obtained using Scanning Electron Microscopy (SEM). Light absorption properties were measured using Ultraviolet-visible diffuse reflectance spectroscopy (UV-Vis DRS) with a measurement range of 200–800 nm. Then the spectrum obtained is processed using the Kubelka-Munk equation to determine the band gap energy.

3 Results and Discussion

Figure 1 showed the diffractogram of $SrBi_4Ti_{3.9}Fe_{0.1}O_{15}$. The results of the comparison of the diffractogram sample and the standard $SrBi_4Ti_{3.9}Fe_{0.1}O_{15}$ at ICSD 51863 showed conformity which indicates that the target compound $SrBi_4Ti_{3.9}Fe_{0.1}O_{15}$ was successfully synthesized, The typical diffractogram peak of the compound $SrBi_4Ti_{3.9}Fe_{0.1}O_{15}$ was found at position 2θ (°) = 17.3, 21.7, 23.2, 27.7, 30.4, 32.9, 39.7, 47.2, 52.3, and 57.1. The sample synthesized using NaCl flux salt found an additional peak at position 2θ (°) = 30.75 that indicated the presence of an impurity compound identical to the peak of the TiO_2 compound that showed the precursors did not react completely.

The reaction process in the MSS occurs in the salt melts phase (at the above melting point of salt). The precursors will diffuse in melted salt and react with each other [9].

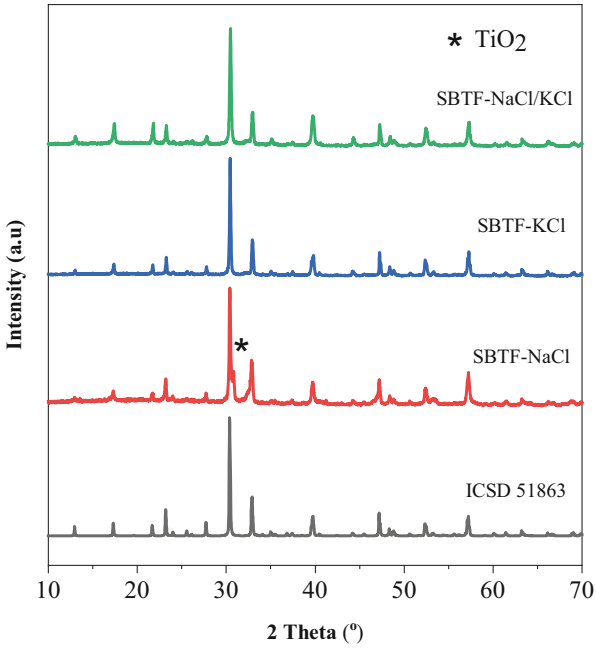

Fig. 1. The diffractogram of $SrBi_4Ti_{3.9}Fe_{0.1}O_{15}$ with various salts

Chang et al. (2014) reported that the samples synthesized using KCl salt completely succeeded in forming the target compound, while the samples synthesized using NaCl salt formed other phases besides the target compound. This can happen because the solubility of TiO_2 in potassium flux is higher than in sodium flux. The solubility relationship between oxide and flux is very important in determining the phase of crystal nucleation [15].

Figure 2 showed the shifting of the peak diffractogram at position 2θ (°) = 30.80 to larger, which indicates the changes in the crystal lattice size due to the addition of Fe dopant, which replaces a small part of the Ti^{4+} cation. The crystal size changes relate to the ionic radii of Fe^{3+} (0.064 nm) with Ti^{4+} [11].

Figure 3 showed the refinement plot of the diffractogram sample of $SrBi_4Ti_{3.9}Fe_{0.1}O_{15}$ synthesized with KCl and NaCl-KCl salts, and the results are summarized in Table 1. The results of the refinement showed that the value of R_p 11.39 and the value of R_{wp} 9.58 for the sample synthesized with KCl salt, while the sample synthesized with NaCl-KCl salt had a value of R_p 10.45 and R_{wp} 9.23. The values of R_p and R_{wp} below 15 indicate that the diffractogram sample has good conformity with the standart.

Figure 4 shoewed the particle morphology of the $SrBi_4Ti_{3.9}Fe_{0.1}O_{15}$ and can be seen that the morphology of all sample is thick plate-like and the particle size is not uniform. It indicate that the particle growth process is similar. Therefore can be considered that

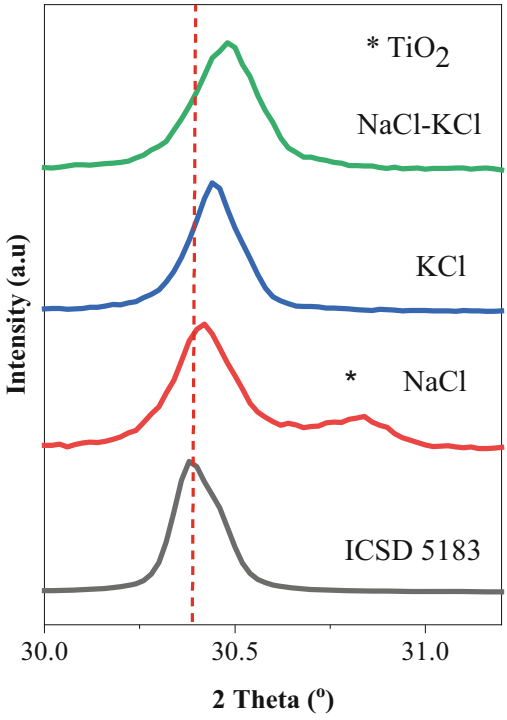

Fig. 2. The Peak position at 2θ (°) = 30.80

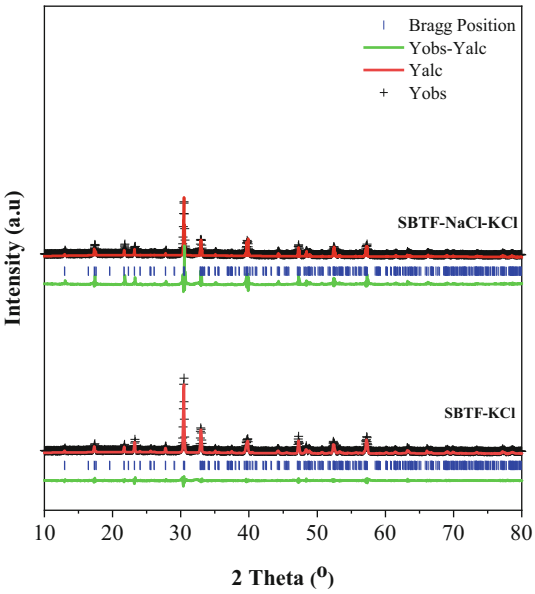

Fig. 3. The refinement plot od $SrBi_4Ti_{3.9}Fe_{0.1}O_{15}$ diffractogram

Table 1. The results of refinement

Parameter	**ICSD No. 51863** $SrBi_4Ti_4O_{15}$	$SrBi_4Ti_{3,9}Fe_{0,1}O_{15}$	
		KCl	**NaCl-KCl**
Crystal System	Ortorombik	Ortorombik	Ortorombik
Space Group	A 21 am	A 21 am	A 21 am
Azimetric Units (Z)	4	4	4
a (Å)	5.4507	5.4516(6)	5.4505(6)
b (Å)	5.4376	5.4284(9)	5.318(8)
c (Å)	40.9841	40.9796(5)	40.9672(4)
Cell Volume (Å)	1214.72	1212.74	1212.89
R_p (%)	–	1.,39	10.45
R_{wp} (%)	–	9.58	9.23
GoF (X^2)	–	0.1951	0.1580

the type of salt used in the synthesis of SBT compounds does not affect the growth of the particles.

Figure 5 showed the reflectance spectrum of SrBi4Ti3.9Fe0.1O15; meanwhile, Fig. 6 showed the Tauc plot of $SrBi_4Ti_{3.9}Fe_{0.1}O_{15}$. The results of the Kubelka-Munk calculation (band gap energy) are summarized in Table 2, and it can be seen that the band gap energy

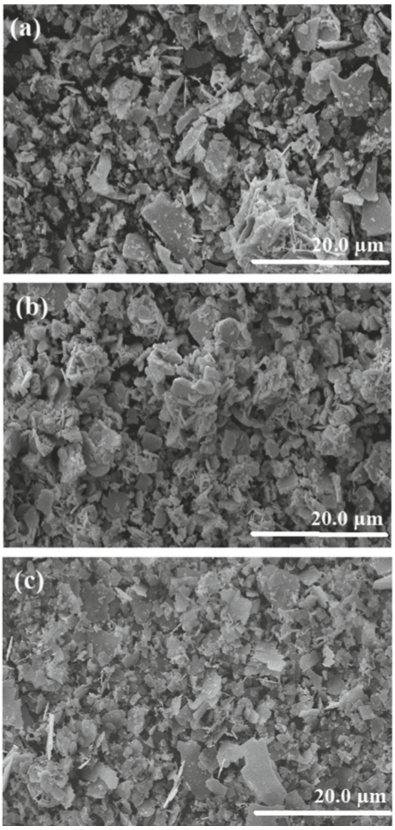

Fig. 4. Micrograph of $SrBi_4Ti_{3.9}Fe_{0.1}O_{15}$ compound with various salts a) NaCl; b) KCl; c) NaCl-KCl

of $SrBi_4Ti_{3.9}Fe_{0.1}O_{15}$ is lower than $SrBi_4Ti_4O_{15}$. It is due to Fe metal as dopants induce absorption shifts into the visible light range by narrowing the band gap [5].

The compound $SrBi_4Ti_4O_{15}$ which has a band gap energy of 3.0 eV was successfully reduced by the addition of Fe dopant energy. The band gap energy value is determined by plotting the photon energy as the *x*-axis and $(F(R).hv)^{1/2}$ as the *y*-axis. The obtained band gap energies are summarized in Table 2.

The lower band gap energy value is related to the rearrangement of the molecular orbitals due to the addition of Fe doping. The electron transition that occurs from the valence band (Bi-6*s* + O-2*p*) to the conduction band (Ti-3*d*) turns into an orbital from the valence band (Bi-6*s* + O-2*p*) to the conduction band (Fe-3*d*) after the addition process Fe doping. This phenomenon occurs due to the charge transfer between Fe^{3+} and Ti^{4+} [4].

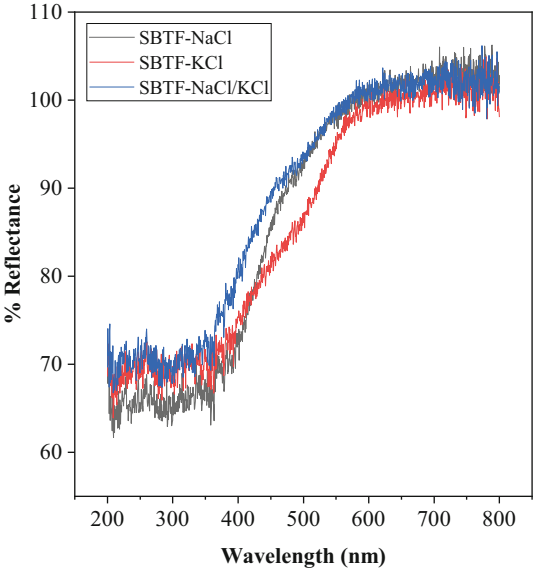

Fig. 5. % Reflectance of $SrBi_4Ti_{3.9}Fe_{0.1}O_{15}$

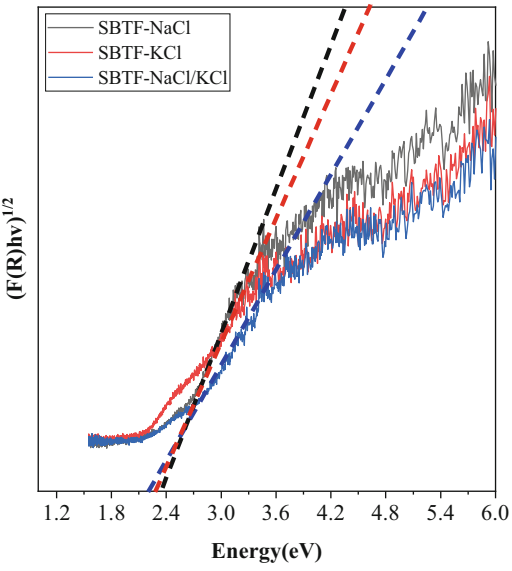

Fig. 6. Plot of Tauc $SrBi_4Ti_{3.9}Fe_{0.1}O_{15}$

Table 2. Band gap energy for $SrBi_4Ti_{3.9}Fe_{0.1}O_{15}$

Compound	Band Gap Energy (eV)	Wavelengt (nm)
$SrBi_4Ti_{3,9}Fe_{0,1}O_{15}$-NaCl	2.31	537
$SrBi_4Ti_{3,9}Fe_{0,1}O_{15}$-KCl	2.27	546
$SrBi_4Ti_{3,9}Fe_{0,1}O_{15}$-NaCl-KCl	2.21	561

4 Conclusion

The compound $SrBi_4Ti_{3.9}Fe_{0.1}O_{15}$ was successfully synthesized using the molten salt method. Sample synthesized using KCl and NaCl-KCl salt have a good crystallinity and purity. $SrBi_4Ti_{3.9}Fe_{0.1}O_{15}$ has a plate-like morphology. All of the salt used in this research can decreased the band gap energy of the sample. So this compound can be used as a photocatalyst material because it has a band gap energy in the range of 2.31–2.21 eV.

References

1. Huang, X. J., Yan, X., Wu, H. Y., Fang, Y., Min, Y. H., Li, W. S., Wang, S. Y., & Wu, Z. J. (2016). Preparation of Zr-doped $CaTiO_3$ with enhanced charge separation efficiency and photocatalytic activity. *Transactions of Nonferrous Metals Society of China (English Edition)*, *26*(2), 464–471.
2. Lee, S., & Park, S. (2013). TiO_2 photocatalyst for water treatment applications. *Journal of Industrial and Engineering Chemistry*, *19*, 1761–1769.
3. Haikal, F., & Prasetyo, A. (2021). Uji Aktivitas Fotokatalis Senyawa Aurivillius Lapis Empat $SrBi_4Ti_4O_{15}$ Dalam Mendegradasi Rhodamine-B. *Al-Kimiya*, *8*(1), 37–41.
4. Liu, Y., Zhu, G., Gao, J., Hojamberdiev, M., Zhu, R., Wei, X., Guo, Q., & Liu, P. (2017). Enhanced photocatalytic activity of $Bi_4Ti_3O_{12}$ nanosheets by Fe^{3+}-doping and the addition of Au nanoparticles: Photodegradation of Phenol and bisphenol A. *Applied Catalysis B: Environmental*, *200*, 72–82.
5. Kanakaraju, D., Hazim Bin Ya, M., Akif Aizuddin Bin Jasni, M., Sufian Bin Endra, M., & Lim, Y. C. (2019). Fe Doped Titania Photocatalyst for Degradation of Methyl Orange. *Materials Today: Proceedings*, *19*, 1657–1662.
6. Gupta, S. K., & Mao, Y. (2021). A review on molten salt synthesis of metal oxide nanomaterials: Status, opportunity, and challenge. *Progress in Materials Science*, *117*(January 2019), 100734.
7. Wendari, T. P., Arief, S., Mufti, N., Insani, A., Baas, J., Blake, G. R., & Zulhadjri. (2020). Structural and multiferroic properties in double-layer Aurivillius phase $Pb_{0.4}Bi_{2.1}La_{0.5}Nb_{1.7}Mn_{0.3}O_9$ prepared by molten salt method. *Journal of Alloys and Compounds*, *820*, 153145.
8. Moure, A. (2018). Review and perspectives of Aurivillius structures as a lead-free Piezoelectric system. *Applied Sciences (Switzerland)*, *8*(1).
9. Xue, P., Wu, H., Lu, Y., & Zhu, X. (2018). Recent progress in molten salt synthesis of low-dimensional perovskite oxide nanostructures, structural characterization, properties, and functional applications: A review. *Journal of Materials Science and Technology*, *34*(6), 914–930.

10. Chen, Z., Jiang, H., Jin, W., & Shi, C. (2016). Enhanced photocatalytic performance over $Bi_4Ti_3O_{12}$ nanosheets with controllable size and exposed {001} facets for Rhodamine B degradation. *Applied Catalysis B: Environmental*, *180*, 698–706.
11. Gu, D., Qin, Y., Wen, Y., Li, T., Qin, L., dan Seo, H. J. 2017. Electronic Structure and Optical Properties of V-doped $Bi_4Ti_3O_{12}$ Nanoparticles. *Journal ofAlloys and Compounds* 695, 2224–2231.
12. Liu, R., Zhan, Y., Liu, L., Liu, Y., & Tu, D. (2020). Morphology analysis and luminescence properties of YVO_4:Sm^{3+},Eu^{3+} prepared by molten salt synthesis. *Optical Materials*, *100*(October 2019), 109633.
13. Nayak, P., & Singh, A. K. (2018). Correlation between orthorhombic distortion with relaxation and Conduction mechanism of Gd^{3+} modified $SrBi_4Ti_4O_{15}$ ceramics. *Ceramics International*, *44*(18), 22840–22849.
14. Wei, J., Li, H., Mao, S., Zhang, C., Xu, Z., & Dkhil, B. (2012). Effect of particle morphology on the photocatalytic activity of $BiFeO_3$ microcrystallites. *Journal of Materials Science: Materials in Electronics*, *23*(10), 1869–1874.
15. Chang, Y., Wu, J., Yang, B., Zhang, S., Lv, T., & Cao, W. (2014). Synthesis and properties of high aspect ratio $SrBi_4Ti_4O_{15}$ microplatelets. *Materials Letters*, 12–15.
16. Jiang, W., Chen, T., Yang, X., Ruan, L., Liu, Y., Meng, X., Xu, G., & Han, G. (2019). Surfactant-Free Synthesis of Single-Crystalline $Bi_4Ti_3O_{12}$ Nanosheets with Excellent Visible-Light Photocatalytic Activity. *Catalysis Surveys from Asia*, *23*(4), 322–331.
17. Zhao, W., Jia, Z., Lei, E., Wang, L., Li, Z., & Dai, Y. (2013). Photocatalytic degradation efficacy of $Bi_4Ti_3O_{12}$ micro-scale platelets over methylene blue under visible light. *Journal of Physics and Chemistry of Solids*, *74*(11), 1604–1607.